Proceedings of the 12th International Conference on
Aluminium Alloys, September 5-9, 2010, Yokohama, Japan

pp. 1324-1329

3D Characterisation and Modelling of Fatigue Damage and Cracking in Metallic Alloys Using X-ray Tomography

J-Y Buffière[1], N Limodin[1], J Réthoré[2], A Gravouil[2], F Hild[3], S Roux[3]

[1]MATEIS, Université de Lyon INSA-Lyon / UMR CNRS 5510, Villeurbanne, France
[2]LAMCOS, Université de Lyon INSA-Lyon / UMR CNRS 5259, Villeurbanne, France
[3]LMT-Cachan, ENS de Cachan / UMR CNRS 8535 / UPMC / PRES UniverSud Paris, Cachan, France

In this paper, the potential of high resolution X-ray micro-tomography is illustrated for the characterisation of damage and cracking developments in structural materials. Fatigue crack initiation and growth has been investigated in metals submitted to various types of loading conditions. Quantitative data are extracted from the three dimensional images and used to test/validate damage and cracking models. The limitations of the technique, in its current state of development, are also shown, giving indications for future developments.

Keywords: *X-ray tomography, cracks, fatigue, digital volume correlation, finite element.*

1. Introduction

X-ray micro-tomography is a technique that enables for the visualization of internal features in opaque samples. Being a non destructive technique, it also allows, in principle, for in situ visualization of damage development. In the last fifteen years, significant progress has been made in terms of resolution with both the availability of third generation synchrotron X-ray sources, new detectors, and affordable (i.e. commercially available) Computed Tomography equipment [1]. A spatial resolution close to that of an optical microscope can now be achieved in 3D that opens (or re-opens) wide areas of research. One of those areas is the 3D characterisation of fatigue cracks.

The scientific issues relevant for such 3D characterisation depends however on whether fatigue cracks are *small* or *long,* a terminology based on the crack size a and its associated plastic zone r_p. Size [2].

Although a lot of experimental and theoretical effort has been spent in the characterisation and modelling of small fatigue crack propagation (see for example Newman [3] for a review), the growth rate predictions for this kind of defects are far from being completely satisfactory for the moment. One very basic problem caused by small fatigue cracks is that their complex three dimensional (3D) shapes affect their propagation behaviour. Therefore the propagation at the surface of a fatigue sample is not necessarily representative of the bulk behaviour, contrary to long cracks. Although this problem has been recognized at least twenty years ago it has hardly been taken into consideration in practice. Design against fatigue in industrial components sometimes includes technical specifications to account for small fatigue crack growth, mainly on the basis of empirical models [4]. The resolution of experimental techniques such as beach marking heat tinting or oxidation is hardly sufficient to visualise the 3D shape of small cracks and the effect of those techniques on the crack propagation rate remains an open issue. Thus, experimental characterisation of the 3D growth of small fatigue cracks has, up to now, remained very limited.

In the case of long cracks, on the other hand, an important issue remains the influence of the stress state (*e.g.* plane stress *vs.* plane strain) on the closure behaviour of cracks. Several Finite Element (FE) models of this phenomenon have been published in recent years [5] but very few of them have been confronted to experimental evidences mainly because of their difficult accessibility.

This paper is a review of experiments carried out in the last eight years at the European Radiation Synchrotron Facility (ESRF). It aims at illustrating the potential of high resolution synchrotron X-ray micro-tomography for the study of fatigue damage development in metallic materials under cyclic loading. The limitations of the technique in terms of *spatial resolution vs. sample size* are underlined and experimental setups/methods are briefly described. The quantitative use of the 3D images for validating/testing fatigue models is illustrated.

2. Experimental

2.1 Tomography

The experiments described in this paper have all been performed at the ESRF in Grenoble (France) on beam line ID19. In the following, we briefly recall some important features that will be used further for discussing the limitations of the technique. The permanent micro-tomographic set-up has been designed to perform experiments giving 3D images with a voxel[i] size ranging from 0.3 µm to several tens of µm according to the optics used. Obtaining a tomographic image consists, first, in recording a series of N radiographs of a sample that is rotated around one axis (generally set vertical). These N radiographs are then used by a reconstruction algorithm to obtain a 3D numerical image of the sample that is, in its classical form, a 3D map of the attenuation coefficient in the sample [6].

The two dimensional (2D) radiographs that compose the tomographic scan of the studied samples are recorded on a detector developed at the ESRF [7]. It consists of a Fast REad out (60 ms), LOw Noise (FRELON) Charge Coupled Device (CCD) camera with a square array of 2048 x 2048 pixels. This detector is coupled with a fluorescent screen via optical lenses. The white beam coming out of the synchrotron ring is rendered monochromatic by a multilayer monochromator. The energy of the beam can be tuned from 10 keV to around 60 keV. The beam coming out of the monochromator is parallel so that no geometric magnification is possible; instead, the voxel size is a result of the optics used.

Another important feature of beam line ID19 is the unusually long source to specimen distance (145 m) that enables phase contrast imaging to be performed in a very simple way by increasing the sample to detector distance.

2.2 Mechanical loading

A dedicated fatigue testing machine with a reduced size and a low vibration level has been designed in order to monitor in situ crack initiation and propagation [8]; it is directly installed on the rotation stage of the micro-tomography setup. The load is transmitted from the top to the bottom of the machine via a thin perspex tube[ii] (1 mm thick, 60 mm in diameter) that allows for a 180 degree rotation without hiding the sample and that results in a *constant but negligible* attenuation of the X rays beam. During a typical fatigue experiment, the samples are cycled in air with a constant stress amplitude ($R = 0.1$). Crack initiation is first monitored by radiography. Once a crack is initiated, full 3D tomographic scans of the crack are recorded at regular intervals during the (interrupted) fatigue test, which is stopped before the final fracture of the sample. During image acquisition the sample is maintained under maximum load to improve crack detection. Hour glass specimens are used (section 1×1 mm^2); in some cases a thin (2 µm) rectangular notch, 100 µm wide and 20 µm deep, was machined in the sample using Focused Ion Beam (FIB). This notch is located at the centre of one of the specimen faces and acts as a crack initiation site [9].

2.3 Limits of the technique

The voxel size required for imaging fatigue cracks under load is of the order of 1 µm. With the parallel beam used on ID19, the maximum size of a sample *whose projections entirely fit on the detector* is directly given by the product of the voxel size in the reconstructed image v_s by the

[i]A voxel is the smallest elementary numerical element composing 3D images. It is therefore the 3D equivalent of the pixel in classical two dimensional images.

[ii]If metallic supports were used as in classical tension/compression rigs, they would hide the sample from the beam during the 180 degree rotation.

number of elements *n* of the CCD detector [1]. For a voxel size of 0.7 μm and the 2048 × 2048 pixel FRELON camera, this gives a maximum sample size of 1.4 mm that corresponds to a square cross section of 1 × 1 mm^2. In a metallic material with a typical grain size of the order of 50- 100 μm this implies that a stable fatigue crack nucleated and propagated *in situ* can at best traverse between 10 to 20 grains and is therefore a *microstructurally small crack*.

Another intrinsic limitation of the tomography technique is the efficiency of the imaging detector at *high energy*. Assuming that the efficiency of the fluorescent screen used for imaging with a 0.7 μm voxel size falls off quickly above an energy of 30 keV, a simple attenuation calculation shows that the maximum sample size that can be imaged while keeping a 10% transmission of the incident beam is 8 mm for Al, and only 1 mm for iron. This result explains why, at the moment, fatigue cracks with a size of several millimetres, are only imaged in 3D at high resolution in light alloys.

Finally, because of the presence of the tube of the fatigue machine mentioned above, the detector to specimen distance cannot be less than 35 mm. For voxel sizes of the order of 1 μm, this distance induces a large amount of phase contrast on the reconstructed images [8,10] If phase contrast does help to underline defects such as cracks and therefore considerably facilitates a visual *on line* detection during an in situ experiment, the presence of diffraction fringes on the crack edges and at the crack tips makes a *quantitative analysis* of the crack shape more difficult [11].

3. Small crack characterisation

3.1 Crack initiation from defects

Fatigue cracks, in their large majority, initiate from defects that create elastic / plastic heterogeneities in the material. A few experimental evidences can be found in the literature that show that this transient process is three dimensional *i.e.* that the development of a microstructurally small crack is difficult to describe from simple surface observations. However no systematic study has been undertaken so far in this field. Some results have been obtained with tomography in the last eight years, for example on cast Al alloys [12-14], or cast iron[15,16]. They show that during uniaxial fatigue the probability of initiating a crack from a porosity-like defect (e.g., microshrinkage cavity) is strongly correlated with the distance of the defect to the surface and that initiation from defects located at a distance greater than the defect size are rarely observed [16]. Another interesting point shown by 3D images is that although nearly all defects intersecting the surface do initiate a crack, most of them will remain non propagating [13], namely, the driving force for microstructurally small crack propagation in the vicinity of the defect being probably high enough for initiation but too low for propagation. Finally, detailed observations of the development of a microstructurally small fatigue crack around a porosity in a cast Al alloy have shown that a substantial part of the fatigue life can be spent in transforming the initiating pore into a crack, a process which is non visible from the surface. During this transient stage, grain boundaries, made visible by a Gallium infiltration technique [12], have also been observed to play a significant role as obstacles that slow down crack propagation [14].

3.2. ***Propagation of microstructurally small cracks***

By using the Ga infiltration technique, it is possible to correlate protruding or retarded parts of 3D crack fronts with the presence of grain boundaries [12,14]. The ability of a microstructurally small crack to propagate faster / slower in some grains is probably linked to the ease / difficulty of activating small scale plasticity in the adjacent grains as suggested, for instance, by Newman [3]. The knowledge of the local crystallographic orientation is necessary to check this assumption. This orientation can now be obtained by Diffraction Contrast Tomography (DCT), a non destructive characterisation technique that is a variant of tomography also developed at ESRF [17]. Preliminary results have been obtained on a Ti alloy. Images of a short fatigue crack propagating in a fully characterised subset of grains (3D shape and orientation) have been obtained. They show that the propagation of a small crack is a highly 3D process and that, because of the continuity of the crack front, the growth of a crack in a given grain is strongly influenced by the difficulty / ease of growing in the neighbouring grains [18].

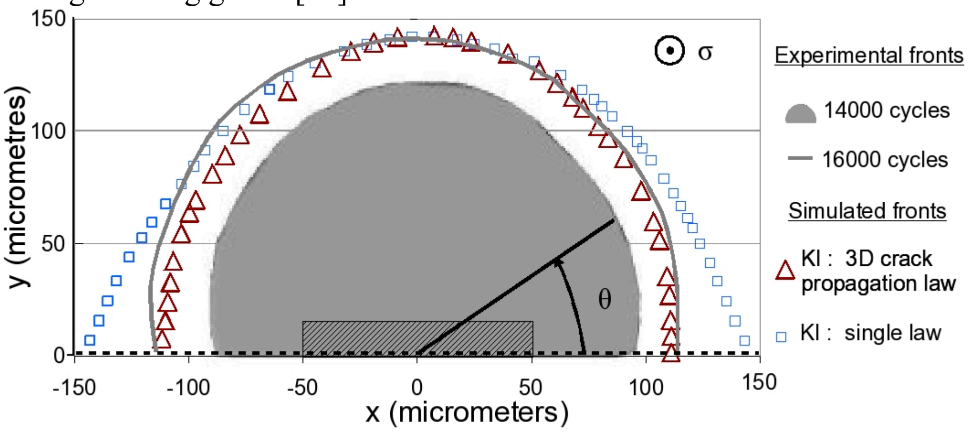

Figure 1 3D rendition of a crack growing in mode I inside a sample of a fine grain (1 µm) Al-Li alloy. The sample surface corresponds to the dashed line ($\theta = 0°$). The crack initiates from an artificial notch machined by FIB (hatched rectangle) [9]. Hollow squares and triangles indicate the simulated crack fronts, respectively without and with crack closure taken into account.

For the reasons given before (i.e., limited field of view) it has not been possible yet to image the transition from the microstructurally small crack regime to the long crack regime. Instead, a simulation of a "long crack" experiment has been carried out on a 5091 Al-Li alloy [9] with an ultra fine grain size (~ 1 µm). The advantage of such a fine microstructure is twofold. First the number of grains encountered by the front of a crack with a typical size of a few hundred µm is comparable to the number of grains encountered by a long (several millimetres) crack in a material with a 50 µm grain size. Second, the crack shape in this kind of material is known to be extremely flat and therefore Finite Element modelling of the crack can be performed.

4. «Long» crack modelling

4.1 FE modelling of 3D propagation.

Figure 1 shows three stages of propagation of a crack that has been initiated from a FIB notch. The profile of the stress intensity factor, *K*, along the crack front of Fig. 1 has been calculated using eXtended 3D Finite Element Method (XFEM) [9]. The FE mesh is directly obtained from the 3D reconstructed image. The local propagation rate along the crack front as defined by the angle θ in Fig. 1 was measured. For $\theta = 90°$ the propagation rate was found to be larger, for equivalent crack sizes, than for $\theta = 0°$ (surface of the sample). It was possible to simulate the experimental crack fronts by a 3D crack growth law da/dN=f(θ) which accounts for a linear variation of the closure level between the surface (maximum closure level) and the bulk (no closure). This variation can in principle be mapped from the reconstructed 3D images as described in the next section.

4.2 Digital volume correlation

Displacement fields resulting from the application of a mechanical load in a material can be assessed, in principle, by measuring the displacement of elements of the microstructure between a reference and a deformed volume. Two different methods, called particle tracking (PT) and digital volume correlation (DVC) can be used. While the first one evaluates the displacements of microstructural features through the motion of their centre of mass, the second one uses correlation techniques to register the two volumes. Both PT and DVC require the presence within the images of markers. Two different strategies have been employed so far. One is to introduce artificially those markers in the studied material [19-20], the other one is to directly use the material microstructure [21-25]. The first method can in principle be applied to a variety of materials, provided a suitable technique for distributing homogeneously the markers is found. However, the question of how much the presence of those features affects the deformation process remains an issue. From that point of view, natural markers appear more attractive, but the number of materials presenting a relevant microstructure is restricted.

These techniques have been used to evaluate the displacement field in the vicinity of the tip of a crack (Figure 2). This then gives a *direct* evaluation of the crack driving force via the extraction of the mixed mode stress intensity factors as explained for example by Rannou *et al.* [25]. This has been done in Al alloys using the marker tracking technique [23] and also in cast iron by using DVC [26]. In this last material, for example, tomography and DVC were used to measure values of the opening stress intensity factor K_{op} and also to correlate crack opening / closure with crack propagation / arrest in comparison with local crack surface roughness.

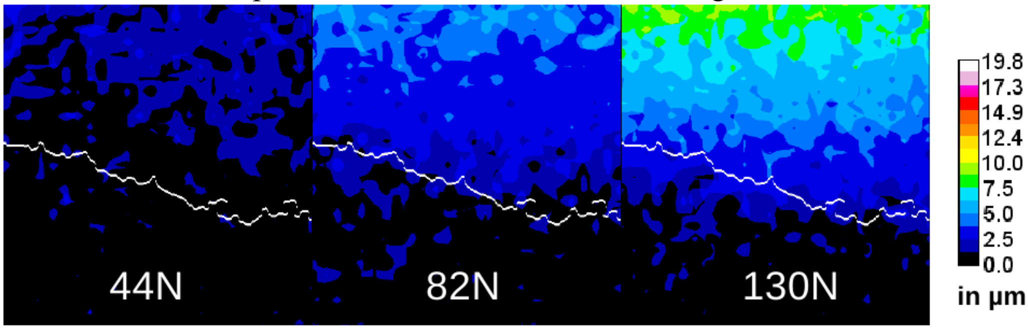

Figure 2 Map of the Crack Opening Displacement (COD) in mode I across the cross section of a cast iron sample for different values of applied load (stress direction perpendicular to the plane of the figure). The white line indicates the position of the crack front (propagation direction from the top towards the bottom of the image). The dark areas observed above the crack front on the left image indicate that for a load of 44N the crack is not open [26].

5. Conclusion

The availability of powerful synchrotron X ray sources coupled with the development of new detectors has enabled for the development of high resolution X ray microtomography setups that provide images of internal features in optically opaque materials with a spatial resolution close to that of optical microscopy. Such studies are for the moment limited to small (~ 1-5 mm^2 cross section) samples mainly in non attenuating materials. In the studies reported here, this technique has been applied to the field of fatigue. The 3D shape of fatigue cracks grown in situ can be determined, thereby providing unique experimental data. In the metals and alloys studied so far, irregularities observed along the crack fronts of microstructurally small cracks are clearly correlated with the presence of grain boundaries. A variant of tomography (DCT) can now provide the successive fronts of a crack growing in a set of fully characterized grains, a key issue in the understanding of small fatigue cracks growth mechanisms. The 3D shape of long cracks appear more regular than that of small cracks and they can thus be modelled using finite element simulations that allow one to extract stress intensity factors values. Those simulations can be very efficiently improved with the use of DVC that enables for a direct evaluation of crack opening / closure and also allows for the extraction of *K* values along the crack fronts, giving direct access to the crack driving force. The comparison of various experimentally and numerically determined data (e.g., crack morphology, crack front, crack opening displacements, stress intensity factors) opens the way for identifying and validating 3D crack propagation models.

Acknowledgements

This work was funded by the CETIM Foundation grant entitled PROPAVANFIS.

References

[1] S. Stock *Micro Computed tomography: methodology and applications*. (CRC Press Toronto 2008).
[2] R.O. Ritchie and J. Lankford: *Small fatigue cracks*, Ed. R.O. Ritchie and J. Lankford (The Metallurgical Society, Warrendale PA,1986) pp.2-5.
[3] J.C. Newman Jr: Progress in Aerospace Science 34 (1998) 347-390.
[4] D.L. McDowell: Eng. Frac. Mech. 56 (1996) 357-377.
[5] R. Branco, D. Rodrigues and F.V. Antunes, Fat. Fract. Eng. Mater. Struct. 31 (2008) 209-216.
[6] A.C. Kak and M. Slaney, *Principles of computerized imaging* (IEEE press, New York,1988).
[7] J-C. Labiche, O. Mathon, S. Pascarelli, M.A. Newton, G. Ferre, C. Curfs, G. Vaughan, A. Homs and D. Fernandez Carreiras: Rev. Sci. Instrum. 78 (2007) 091301.
[8] J.-Y. Buffiere, E. Maire, J. Adrien,·J.-P. Masse and E. Boller: Exp. Mech. 50 (2010) 289–305.
[9] E. Ferrie, J.Y. Buffière, W. Ludwig, A. Gravouil and L. Edwards: Acta Mater. 54 (2006) 1111-1122.
[10] P. Cloetens, M. Pateyron-Salomé, J.Y. Buffière, G. Peix, J. Baruchel, F. Peyrin and M. Schlenker: Jal. Appl. Phys. 81 (1997) 5878-5886.
[11] J-Y. Buffiere, E. Ferrie, H. Proudhon, and W. Ludwig: Mater. Sci Technol. 22 (2006) 1019-1024.
[12] W. Ludwig, J.Y. Buffière, S. Savelli and P. Cloetens: Acta Mater. 51 (2003) 585-598.
[13] J.Y. Buffiere, S. Savelli, P.H. Jouneau, E. Maire and R. Fougères: Mat. Sc. Eng. A 316 (2001) 115-126.
[14] E. Ferrié, J.Y. Buffière and W. Ludwig: Int. Jal. Fatigue 27 (2005) 1215-1220.
[15] T.J. Marrow, J.Y. Buffière, P.J. Withers, G. Johnson and D. Engelberg: Int. Jal. Fatigue 26 (2004) 717-725.
[16] C. Verdu, J. Adrien and J-Y. Buffiere: Mat .Sc. Eng. A 483 (2008) 402–405.
[17] W. Ludwig, P. Reischig, A. King, M. Herbig, E.M. Lauridsen, G. Johnson, T.J. Marrow and J-Y. Buffiere: Rev. Sci. Instrum. 80 (2009) 033905.
[18] M. Herbig, A. King, W. Ludwig and J-Y. Buffiere: Acta Mater. 2010 *Submitted*.
[19] S.F. Nielsen, H.F. Poulsen, F. Beckmann, C. Thorning and J.A. Wert: Acta Mater. 51 (2003) 2407-2415.
[20] B.K. Bay, T.S. Smith, D.P. Fyhrie and M. Saad: Exp. Mech. 39 (1999) 217-225.
[21] K. Haldrup, S.F. Nielsen and J.A. Wert: Exp. Mech. 48 (2008) 199-206.
[22] S. Roux, F. Hild, P. Viot and D. Bernard: Composites Part A 39 (2008) 1253-1257.
[23] H. Toda, I. Sinclair, J.Y. Buffiere, E. Maire, K.H. Khor, P. Gregson and T. Kobayashi: Acta Mater. 52 (2004) 1305-1312.
[24] E. Verhulp, B. van Rietbergen and R. Huiskes: J. Biomech. 37 (2004) 1313-1319.
[25]. J. Rannou, N. Limodin, J. Rethore, A. Gravouil, M.C. Baietto-Dubourg, J.Y. Buffiere, A. Combescure, F. Hild and S. Roux: Comp. Meth. Appl. Mech. Eng. 199 (2010) 1307–1325.
[26] N. Limodin, J. Rethore, J-Y. Buffiere, A. Gravouil, F. Hild and S. Roux: Acta Mater 57 (2009) 4090–4101.